Electronic Supplementary Information

Design and synthesis of 3-D hierarchical molybdenum dioxide/nickel/carbon structured composite with superior cycling performance for lithium ion batteries

Qing Xia[1], Hailei Zhao[1,2,*], Zhihong Du[1], Zijia Zhang[1], Shanming Li[4], Chunhui Gao[1], Konrad Świerczek[3]

[1]School of Materials Science and Engineering, University of Science and Technology Beijing, Beijing 100083, China

[2]Beijing Key Lab of New Energy Materials and Technology, Beijing 100083, China

[3]AGH University of Science and Technology, Faculty of Energy and Fuels, Department of Hydrogen Energy, al. A. Mickiewicza 30, 30-059 Krakow, Poland

[4]Beijing National Laboratory for Condensed Matter Physics, Institute of Physics, Chinese Academy of Sciences, P.O. Box 603, Beijing 100190, China

* Corresponding author:

E-mail address: hlzhao@ustb.edu.cn

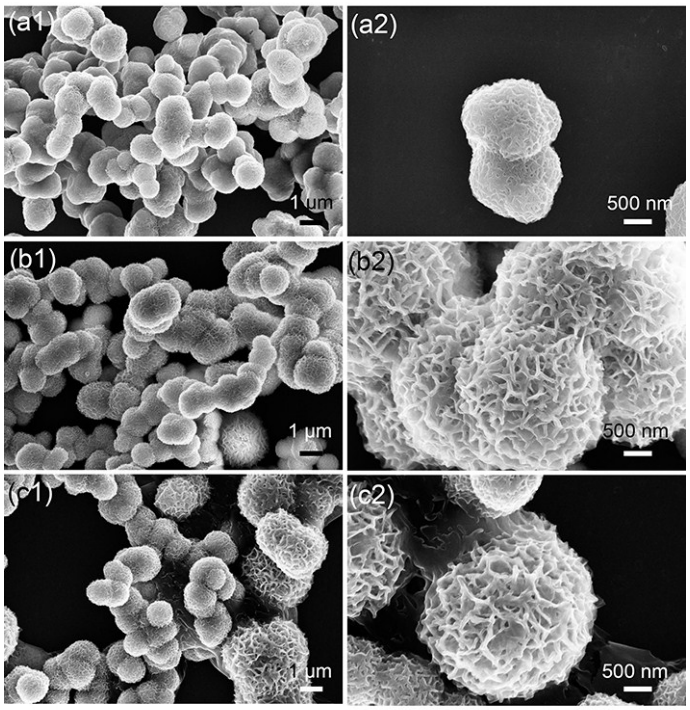

Figure S1. FESEM images of precursor with Ni/Mo = 1 in atomic ratio after different reaction time (a) 1 hour; (b) 1.5 hours; (c) 2 hours.

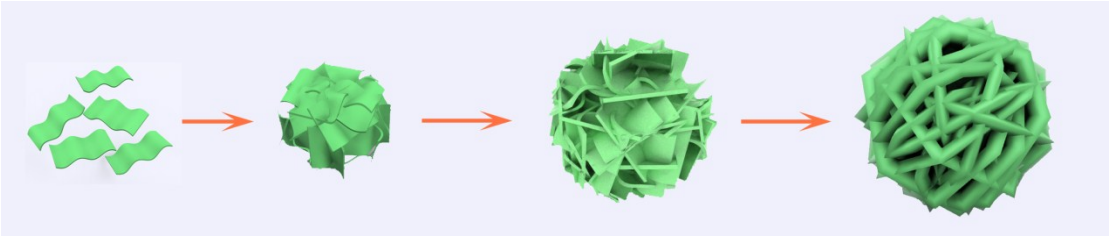

Figure S2. Schematic illustration of the formation process of 3-D hierarchical MoO_2/Ni/C precursor.

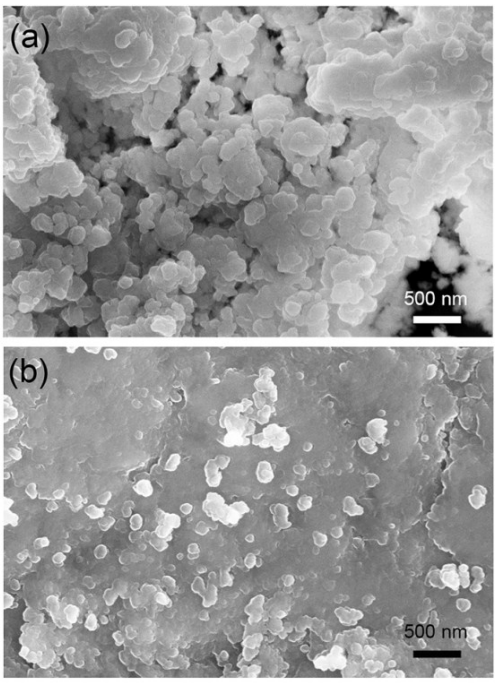

Figure S3. FESEM images of precursor synthesized under conditions with atomic ratio of Ni/Mo = 0.5 (a); Ni/Mo = 0.2 (b).

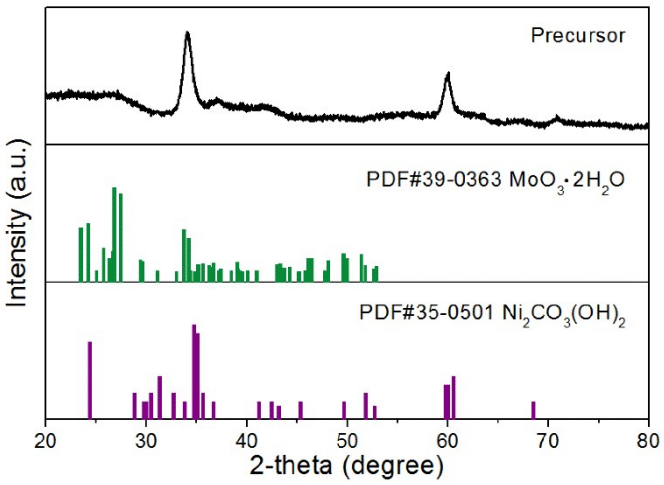

Figure S4. XRD pattern of the precursor prepared under Ni/Mo=1 in atomic ratio at 120 °C for 12 h. The standard spectra are also provided.

According to XRD result of the precursor, the relevant reaction process can be reasoned as Eqs. S(1)-(3):

$$H_2NCONH_2 + 2H_2O \rightarrow NH_4^+ + CO_3^{2-} \quad (1)$$

$$Ni^{2+}+CO_3^{2-}+2H_2O \rightarrow Ni_2CO_3(OH)_2 + 2H^+ \quad (2)$$

$$Mo_7O_{24}^{6-} + 6H^+ + 11H_2O \rightarrow 7MoO_3 \cdot 2H_2O \quad (3)$$

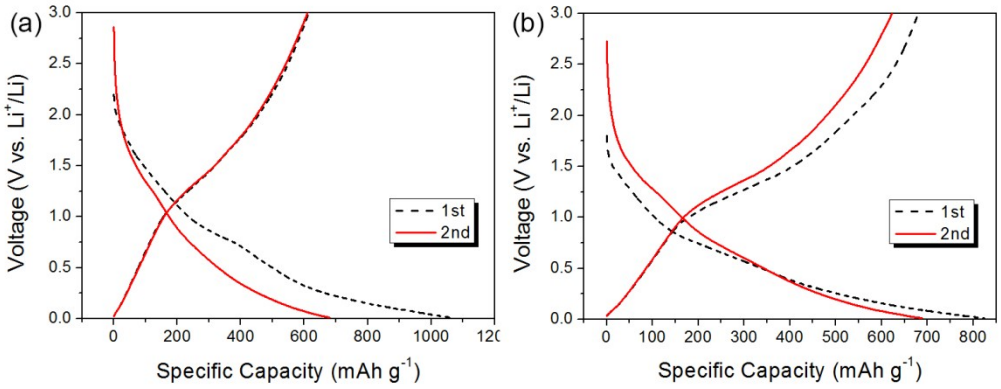

Figure S5. Discharge/charge voltage profiles of MoO_2/Ni/C electrode for the first two cycles: (a) as prepared MoO_2/Ni/C electrode and (b) after pre-lithiation treatment. The pre-lithiation was performed by placing the electrode directly onto the lithium foil and immersing them in electrolyte for 1 hour. The initial coulombic efficiency was improved from 60% to 85%. The initial discharge capacity could be adjusted by treatment time.

Table S1. Comparison of electrochemical performance of the MoO_2/Ni/C electrodes with other reported MoO_2-based electrodes.

Samples	Initial coulombic efficiency (%)	Current rates (mA g^{-1})	Reversible capacities (mA h^{-1})	Cycle Numbers (n)	Ref.
This work	60	100	618	50	
		1000	445	800	
MoO_2-OMC	61.4	50	689	50	S1
MoO_2/Graphene	47	540	550	1000	S2
		1042	497	50	
MoO_2 nanorods	67.2	41.9	830	29	S3
MoO_2-3DG	79.3	50	986.9	150	S4

W-doped MoO_2	76	0.1C	697	20	S5
		2C	180		
MoO_2@C	60	100	617.2	30	S6
		1000	326.6	30	
MoO_2@carbon	85.1	419	800	100	S7
MoO_2/C	52.2	200	629	50	S8
MoO_2/Graphite	58	100	726	30	S9
MoO_2/Mo_2C	85.8	1000	510	140	S10
MoO_2@C-HMS	78.6	100	680	80	S11
		1000	455		
MoO_2/MWCNT	55	100	1143	200	S12
		1000	408		
MoO_2/Graphene	73	1000	597.9	70	S13
MoO_2-GO	73.6	100	523.7	30	S14
MoO_2/C	70.5	200	692.5	80	S15
		400	537.6	475	
Ni:MoO_2	67.4	300	400	80	S16
MoO_2@C	~56	50	762.7	50	S17
MoO_2 monolith		200	719.1	20	S18
MoO_2-graphene	71.5	47.8	71.5	100	S19
MoO_2/C	~62.5	100	602	600	S20
		800	409	50	
Yolk-shell	91.7	50	847.5	50	S21
MoO_2		2000	450		

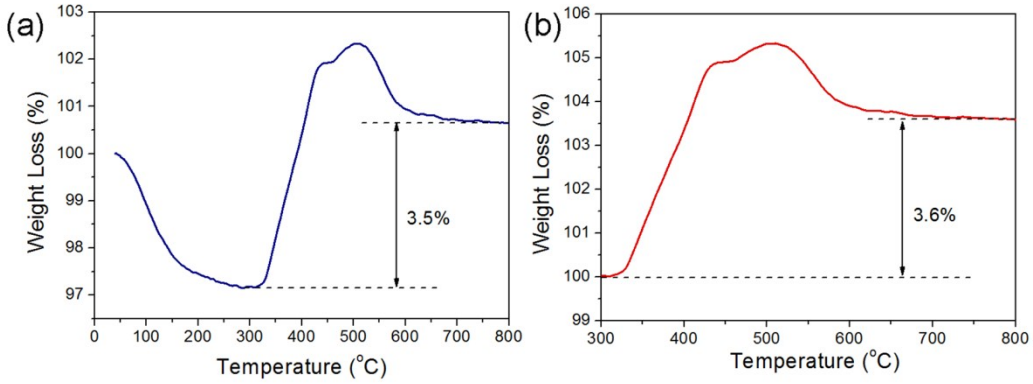

Figure S6. TG original curve (a) and normalized curve (b) of MoO_2/Ni/C composite recorded in air.

Fig. S6 shows the TG curve of MoO_2/Ni/C composite in air. The possible oxidation reactions of MoO_2/Ni/C composite in air are shown in Eqs. (4)-(6).

$$MoO_2 + 0.5O_2 = MoO_3 \quad (4)$$

$$Ni + 0.5O_2 = NiO \quad (5)$$

$$C + O_2 = CO_2 \quad (6)$$

The theoretical value of the weight gain from MoO_2 to MoO_3 is 12.5%, while that from Ni to NiO is 27.3%. After heating in air to 800 °C, the composite experiences weight gain and then weight loss. After 700 °C, the weight tends to be unchanged. The fast weight loss to 150 °C and the followed slow weight loss to 300 °C are due to the evaporation of absorbed water or other solvent groups. The weight gain in the range of 300-500 °C is resulted from the oxidation of MoO_2 and Ni, while the weight loss from 500 to 600 °C comes from the oxidation of carbon. Taking the weight at 300 °C as basic line of MoO_2/Ni/C system, the TG curve is normalized and the resultant plot is shown in Fig. S6b. The total weight gain is 3.6%. Combined with the atomic ratio of Mo/Ni from EDX results, the MoO_2, Ni, and carbon contents in the composite are calculated to be about 61 wt%, 28 wt% and 11 wt%, respectively.

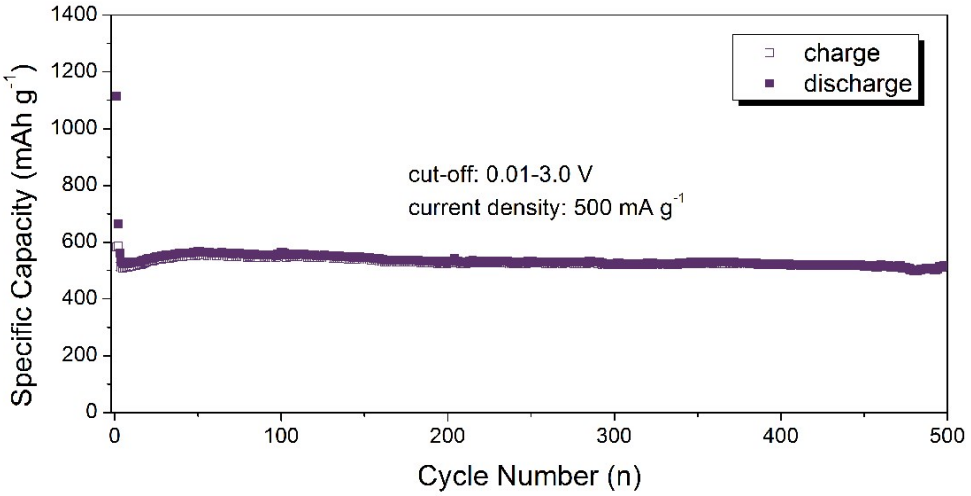

Figure S7. Cycling performance of MoO_2/Ni/C electrode at a current density of 500 mA g^{-1}.

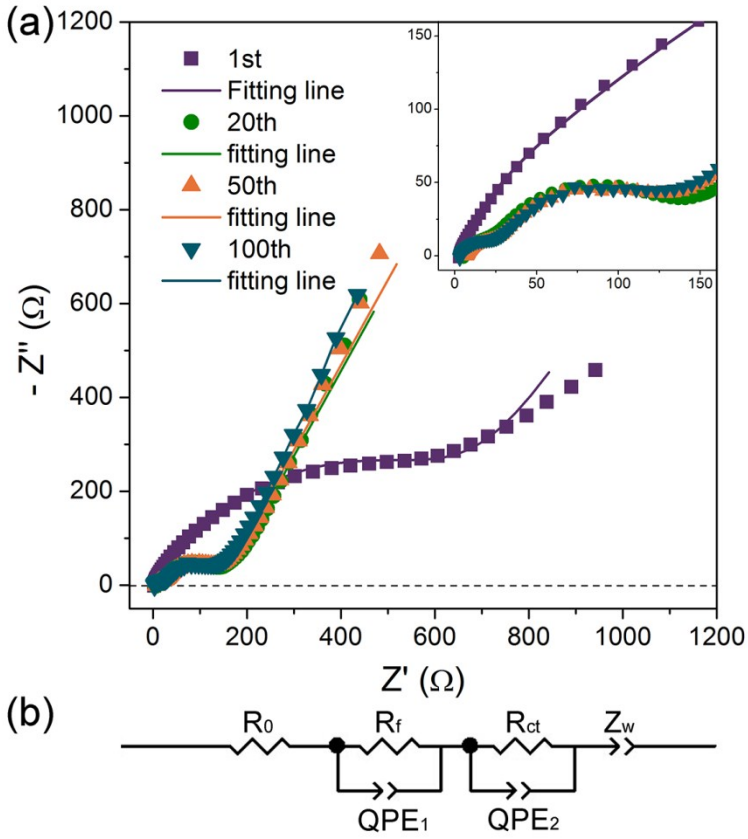

Figure S8. Fitting results of Nyquist plots of the MoO_2/Ni/C electrode after different cycles over the frequency range (a); the equivalent circuit used to fit the experimental impedance spectra (b).

Table S2. Fitting values of R_f and R_{ct} after different cycles.

	1st	20th	50th	100th
R_f (Ω)	3.83	15.65	16.96	23.42
R_{ct} (Ω)	587	128.6	119.3	116.1

References

[S1] L. Zeng, C. Zheng, C. Deng, X. Ding, and M. Wei, *ACS Appl. Mater. Interfaces*, 2013, **5**, 2182–2187.

[S2] A. Bhaskar, M. Deepa, T.N. Rao, and U.V. Varadaraju, J. Power Sources, 2012, **216**, 169–178.

[S3] B. Guo, X. Fang, B. Li, Y. Shi, C. Ouyang, Y.-S. Hu, Z. Wang, G. D. Stucky, and L. Chen, *Chem. Mater.*, 2012, **24**, 457–463.

[S4] Z.X. Huang, Y. Wang, Y.G. Zhu, Y. Shi, J.I. Wong, and H.Y.. Yang, *Nanoscale*, 2014, **6**, 9839–9845.

[S5] X. Fang, B. Guo, Y. Shi, B. Li, C. Hua, C.Yao, Y. Zhang, Y.-S. Hu, Z. Wang, G.D. Stucky, and L. Chen, *Nanoscale*, 2012, **4**, 1541–1544.

[S6] L.Yang, L. Liu, Y. Zhu, X. Wang, and Y. Wu, *J. Mater. Chem.*, 2012, **22**, 13148–13152.

[S7] X. Liu, D. Wu, W. Ji, and W Hou, *J. Mater. Chem. A*, 2015, **3**, 968–972.

[S8] L. Zhou, H.B. Wu, Z. Wang, and X.W. Lou, *ACS Appl. Mater. Interfaces*, 2011, **3**, 4853–4857.

[S9] Y. Xu, R. Yi, B. Yuan, X. Wu, M. Dunwell, Q. Lin, L. Fei, S. Deng, P. Andersen, D. Wang, and H. Luo, *J. Phys. Chem. Lett.*, 2012, **3**, 309–314.

[S10] H.J. Zhang, K.X. Wang, X.Y. Wu, Y.M. Jiang, Y.B. Zhai, C. Wang, X. Wei, and J.S. Chen, *Adv. Funct. Mater.*, 2014, **24**, 3399–3404.

[S11] X. Liu, W. Ji, J. Liang, L. Peng, and W. Hou, *Phys. Chem. Chem. Phys.*, 2014, **16**, 20570–20577.

[S12] A. Bhaskar, M. Deepa, and T. N. Rao, *ACS Appl. Mater. Interfaces*, 2013, **5**, 2555–2566.

[S13] Y. Sun, X. Hu, W. Luo, and Y. Huang, *ACS Nano*, 2011, **5**, 7100–7107.

[S14] S. Hu, F. Yin, E. Uchaker, W. Chen, M. Zhang, J. Zhou, Y. Qi, and Guozhong Cao, *J. Phys. Chem. C*, 2014, **118**, 24890–24897.

[S15] B. Liu, X. Zhao, Y. Tian, D. Zhao, C. Hu, and M. Cao, *Phys. Chem. Chem. Phys.*, 2013, **15**, 8831–8837.

[S16] O. Hirsch, G. Zeng, L. Luo, M. Staniuk, P. M. Abdala, W. Beek, F. Rechberger,

M.J. Süess, M. Niederberger, and D. Koziej, *Chem. Mater.*, 2014, **26**, 4505–4513.

[S17] W. Luo, X. Hu, Y. Sun, and Y Huang, *Phys. Chem. Chem. Phys.*, 2011, **13**, 16735–16740.

[S18] Y. Sun, X. Hu, J.C. Yu, Q. Li, W. Luo, L. Yuan, W. Zhang, and Y. Huang, *Energy Environ. Sci.*, 2011, **4**, 2870–2877.

[S19] F. Xia, X. Hu, Y. Sun, W. Luo, and Y. Huang, *Nanoscale*, 2012, **4**, 4707–4711.

[S20] Y. Sun, X. Hu, W. Luo, and Y. Huang, *J. Mater. Chem.*, 2012, **22**, 425–431.

[S21] X. Zhang, X. Song, S. Gao, Y. Xu, X. Cheng, H. Zhao, and L. Huo, *J. Mater. Chem. A*, 2013, **1**, 6858–6864.